CITE-WHILE-YOU-GENERATE: TRAINING-FREE EVIDENCE ATTRIBUTION FOR MULTIMODAL CLINICAL SUMMARIZATION

Anonymous authors Paper under double-blind review

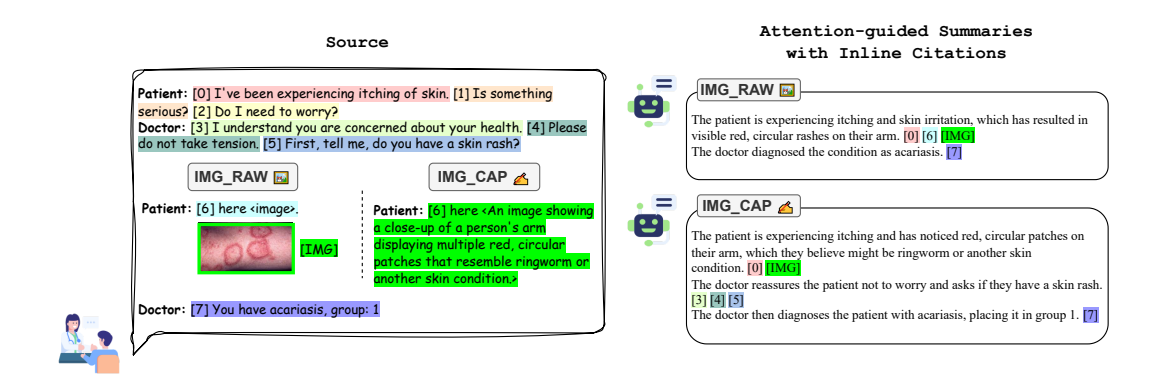


Figure 1: Overview of our proposed framework for inference-time source attribution in clinical summarization. Given a dialogue and an associated image, our method produces summaries with explicit citations to supporting evidence. We support two modes within the same framework: in the IMG_RAW mode, decoder attentions over image patches are directly aggregated to attribute visual evidence, whereas in the IMG_CAP mode, the image is converted into a one-sentence caption to enable purely text-based alignment. Each generated summary sentence is annotated with citations to source text spans and/or the image, providing interpretable and trustworthy clinical summaries.

ABSTRACT

Trustworthy clinical summarization requires not only fluent generation but also transparency about where each statement comes from. We propose a training-free framework for generation-time source attribution that leverages decoder attentions to directly cite supporting text spans or images, overcoming the limitations of post-hoc or retraining-based methods. We introduce two strategies for multimodal attribution: a raw image mode, which directly uses image patch attentions, and a caption-as-span mode, which substitutes images with generated captions to enable purely text-based alignment. Evaluations on two representative domains: clinician-patient dialogues (CLICONSUMMATION) and radiology reports (MIMIC-CXR), show that our approach consistently outperforms embedding-based and self-attribution baselines, improving both text-level and multimodal attribution accuracy (e.g., +15% F1 over embedding baselines). Caption-based attribution achieves competitive performance with raw-image attention while being more lightweight and practical. These findings highlight attention-guided attribution as a promising step toward interpretable and deployable clinical summarization systems.

1 Introduction

Multimodal large language models (MLLMs) are increasingly applied to clinical summarization tasks, where long dialogues or imaging reports must be distilled into concise, actionable notes. These systems promise to reduce documentation burden, improve continuity of care, and accelerate

information retrieval for clinicians. Recent advances in instruction-tuned models have yielded highly fluent summaries, often rivaling or surpassing supervised baselines on automatic metrics.

However, fluency is not enough. MLLMs remain prone to *hallucinations*: claims that are weakly supported or unsupported by the underlying evidence. In high-stakes domains such as radiology and patient documentation, this problem is particularly acute: an unsupported statement about a lesion or a misattributed patient complaint can lead to delayed diagnosis, unnecessary tests, or erosion of clinician trust. For real-world adoption, practitioners require not only concise summaries but also *traceability*: a clear indication of where each statement originated in the source material. Transparency is thus a prerequisite for safe deployment of summarization models in healthcare.

Unfortunately, existing approaches provide limited solutions. Current clinical summarization systems typically output text-only summaries without citations. Post-hoc interpretability tools (Xu et al., 2023; Agarwal et al., 2022) can highlight relevant spans or patches, but they often operate at coarse granularity, do not align well with human-interpretable units such as sentences, and require additional models or retraining that are impractical in hospital workflows. Embedding-based retrieval (Karpukhin et al., 2020; Khattab & Zaharia, 2020) can approximate alignments, yet such methods conflate semantic similarity with factual grounding and struggle when visual evidence is involved. As a result, there remains a gap between what MLLMs produce and the kind of accountable, expect.

We address this gap with a **training-free**, **attention-guided attribution framework** that produces sentence- and image-level citations *during generation*. Our approach leverages decoder attention tensors to map generated tokens back to their most influential source spans, thereby constructing a structured citation map in real time. Unlike post-hoc explanations, this design integrates attribution directly into the generative process, ensuring that evidence is available alongside every generated statement.

As illustrated in Figure 1, we explore two complementary modes for multimodal inputs: (i) *raw image attribution*, which links output tokens directly to image patch embeddings, enabling faithful visual grounding; and (ii) *caption-as-source attribution*, which substitutes model-generated captions for image placeholders, allowing the system to align purely in text space when raw images are unavailable or impractical to share. Together, these modes support both high-fidelity grounding and lightweight deployment.

We evaluate our method in two representative clinical domains: (i) doctor–patient dialogues (CLICONSUMMATION (Tiwari et al., 2023)), which include both text-only encounters and cases with embedded image references, enabling evaluation of sentence- and image-level attribution in multimodal summarization; and (ii) radiology reports (MIMIC-CXR (Johnson et al., 2019)), where we focus on the FINDINGS \rightarrow IMPRESSION summarization task, a standard benchmark for clinical reasoning with free-text inputs.

Using two state-of-the-art open MLLMs Qwen2.5-VL (Bai et al., 2025) and LLaVA-NeXT (Liu et al., 2024), we benchmark our framework against strong baselines including embedding-based similarity and model self-attribution. Across both domains, our method yields higher precision, stronger exact-match performance, and more robust handling of multimodal evidence. Beyond numerical gains, our approach highlights how attention distributions, often dismissed as noisy, can be systematically aggregated into clinically meaningful attributions.

Our contributions are threefold:

- 1. We propose the first training-free method that produces *fine-grained multimodal citations during generation*, aligning output sentences with supporting text spans and images.
- 2. We introduce two complementary strategies for visual attribution: raw image mode and caption-assource mode, highlighting trade-offs between fidelity and efficiency.
- 3. We demonstrate consistent improvements over strong baselines on two clinical summarization benchmarks, providing insights into how attention-guided attribution can enhance the trustworthiness, transparency, and deployability of MLLMs in healthcare.

2 RELATED WORK

Source Attribution Early work on faithfulness for abstractive summarization highlighted how models often produce unsupported content and motivated evidence-grounded evaluation and training signals. Representative evaluation frameworks include SummaC (Laban et al., 2022), which compares summary-source entailment with NLI-style consistency checks, and downstream factuality probes such as SelfCheckGPT (Manakul et al., 2023) that estimate hallucination risk via self-consistency checks. Directly linking generated text to its provenance has gained traction. Traceable Text (Kambhamettu et al., 2024) introduces phrase-level provenance links that attach source spans to generated spans, enabling fine-grained, inspectable justifications. Closer to our setting, Suhara & Alikaniotis (2024) formulates source identification for abstractive summarization, assigning each generated sentence to supporting source sentences, which we extend to the multimodal case with fine-grained sentence-level attributions. Beyond summarization, causal tracing work such as Meng et al. (2022) identifies neuron activations that are decisive in GPT models' factual predictions by corrupting inputs or altering internal activations, and demonstrates how factual associations can be edited once their storage locations in the network are identified. This line of research underscores the broader importance of linking outputs back to internal mechanisms or provenance signals, which we operationalize here via attention-guided attribution.

Summarization in Clinical Settings Radiology and broader clinical summarization raise uniquely high-stakes requirements for faithfulness and transparency. Surveys of radiology report generation/summarization (Sloan et al., 2024) emphasize persistent gaps in factual grounding and clinical utility, calling for methods that surface supporting evidence and reduce hallucinations. Task-driven work in radiology (e.g., pragmatic report generation that conditions on indications/prior studies (Nguyen et al., 2023)) demonstrates that integrating structured context can improve clinical relevance, but interpretability often remains post hoc or coarse-grained. Beyond X-ray, the clinical NLP community has developed entity/relation resources, such as RadGraph (Jain et al., 2021), to enable the structured evaluation of factual correctness. Additionally, DocLens (Xie et al., 2024) includes attribution as one of the dimensions for evaluation.

Multimodal Summarization Multimodal summarization encodes visual inputs with CNN/ViT backbones and fuses them with language via cross-modal attention or gated fusion; however, many systems empirically under-weight images compared to accompanying text. Classic datasets and benchmarks include MSMO (Zhu et al., 2018) and VMSMO (Li et al., 2020), which catalyzed methods that align salient visual regions with summary content. Topic-aware modeling and improved cross-modal attention have been explored to better select image evidence (Mukherjee et al., 2022). Recent work explicitly argues for giving images a stronger influence during summarization: Xiao et al. (2025) emphasizes image-oriented objectives to mitigate text dominance in multimodal summaries. In contrast to these approaches, our goal is complementary: we *instrument* open multimodal LLMs to expose attentions, aggregating them into sentence- and image-level attributions that can be visualized and evaluated, thereby providing provenance signals during summarization rather than only post-hoc checks.

3 Метнор

We present an attention-guided attribution framework that produces fine-grained citations during summarization. Our design balances three goals: *fidelity* (faithfully mapping generated statements to evidence), *efficiency* (training-free inference without auxiliary models), and *generality* (supporting both text-only and multimodal inputs among different models).

At its core, the method is a **single pipeline** that operates on any input: a clinical dialogue, a radiology report, or a multimodal input with images. The pipeline is training-free and leverages cross-attention weights that are already available in decoder-only transformers to construct sentence-level and imagelevel attributions. Text-only and multimodal cases are handled through the same three-stage process, with only the treatment of visual tokens differing between modes.

3.1 PROBLEM SETUP

Here, we define our task of clinical summarization with source attribution. Given a source document D, which may be text-only or multimodal, and a generated summary G, the goal is to attribute each summary sentence $g_j \in G$ to one or more evidence units in D. For text-only inputs, evidence units are source sentences $\{s_1, \ldots, s_{|S|}\}$. For multimodal inputs, the evidence set is augmented with an image element s_{img} . The output is a mapping:

$$\mathcal{A}: \{1, \dots, |G|\} \ \to \ 2^{\{1, \dots, |S|\} \cup \{s_{\rm img}\}},$$

which specifies, for each generated sentence index j, the subset of source sentences (and possibly the image) that support it.

3.2 Core Pipeline

The central challenge in attention-based attribution is how to turn noisy, token-level attention weights into stable and interpretable citations. Raw attention distributions vary across layers, heads, and even tokens within the same sentence, so a direct visualization is not reliable. Our key mechanism addresses this by defining a principled mapping: every generated token is assigned to top-k source sentences through majority voting, and sentence-level attributions are then aggregated through normalized thresholding.

Formally, let $\bar{\mathbf{a}}_t \in \mathbb{R}^K$ denote the pooled attention distribution from a generated token y_t to all source tokens $\{x_1, \dots, x_K\}$. For each token y_t , we collect the top-k attended source tokens, map them to their corresponding sentence IDs, and assign the token to the majority-vote sentence label: $\hat{s}(t)$. For a generated sentence g_i with tokens T_i , we then aggregate token labels with a normalizing threshold τ :

$$\mathcal{A}(j) = \left\{ i : \left(\frac{1}{|T_j|} \sum_{t \in T_j} I[\hat{s}(t) = i] \right) \ge \tau \right\}.$$

This yields the set of supporting sources A(j), ensuring that each generated sentence is attributed only to input sentences (or image spans) that receive consistent support across its tokens.

Our approach is deliberately training-free, requiring no parameter updates or auxiliary models. Instead, it leverages information that every transformer-based decoder already produces: cross-attention weights between generated tokens and source tokens. To transform these raw weights into meaningful citations, we follow a three-stage pipeline common to all input modes: (TEXT, IMG_RAW, IMG_CAP).

- 1. **Chunking.** The first step is to segment the source document into units of evidence that align with how clinicians reason about information. For text-only inputs, this means splitting the document into sentences and assigning each source token to the sentence it belongs to. For multimodal cases, we extend the evidence set by either retaining image placeholders (IMG_RAW) or replacing them with textual captions (IMG_CAP). This ensures that later stages of the pipeline can operate at sentence-level granularity, which is more interpretable to clinicians than token-level alignment.
- 2. **Attention pooling.** Transformers produce a large number of attention heads and layers, each of which may highlight different parts of the input. Rather than relying on a single head, which can be unstable, we average attention scores across all layers and heads for each generated token. This pooling yields a robust estimate of how strongly each output token attends to each input token. Importantly, it also ensures that our framework can be applied to different models without hand-tuning, since the averaging step normalizes away idiosyncrasies of specific architectures.
- 3. **Mapping and aggregation.** The final stage maps token-level attributions into sentence-level citations and filters out spurious alignments. For every generated sentence, we aggregate the source labels of its tokens and apply a threshold τ to decide which sources are retained. This prevents noise from a few stray tokens from being misinterpreted as evidence and guarantees that only sources with consistent support are considered citations. From a clinical perspective, this filtering step is crucial: it avoids overwhelming users with false positives and ensures that every citation shown in the final summary reflects a substantial alignment between the generated content and the source material.

```
216
                       :\mathcal{D}: items with source S and optional image IMG
217
            Input
                      : model M (output_attentions = True), processor P, mode \in \{\text{TEXT}, \text{IMG\_RAW}, \text{IMG\_CAP}\}, top-k,
218
                        thresholds \tau
219
           Output: Per-sentence citations \mathcal{A} and summaries G
220
           foreach item (S, \mathsf{IMG}) \in \mathcal{D} do
221
                 /* --- Prompting and generation ---
                                                                                                                                          */
222
                 if IMG\_RAW then prompt \leftarrow (image, S);
223
                 else if IMG\_CAP then c \leftarrow M.caption(IMG);
224
                 replace <image> in S by \langle c \rangle; prompt \leftarrow S;
225
                 else prompt \leftarrow S // text-only inputs;
226
                 (G, \{\mathbf{A}_t\}) \leftarrow M.generate(P(\mathsf{prompt}), \mathsf{greedy}, \mathsf{attn} = "eager");
227
228
                 /* --- Chunking and alignment ---
229
                 \mathcal{C}_S \leftarrow \texttt{SentenceChunks}(S), \text{ if } \textit{IMG\_RAW then record image token block } I; \texttt{shift indices in } \mathcal{C}_S \texttt{ past}
230
                 \mathcal{C}_G \leftarrow \text{SentenceChunks}(G);
231
                 if IMG_CAP then i^* \leftarrow \text{CaptionSid}(S, \mathcal{C}_S, c);
232
233
                 /* --- Generated Token to source (pooled attention) ---
                                                                                                                                          */
234
                 foreach generated token y_t do
235
                      \bar{\mathbf{a}}_t \leftarrow \operatorname{mean}_{\ell,h,q}(\mathbf{A}_t^{(\ell,h)}[q,:]);
                      ; // \ell: average over layer, head, query to get a single attention
237
                       vector over source tokens
238
                      \hat{s}(t) \leftarrow \text{majority}(\text{topk\_text}(\bar{\mathbf{a}}_t, k) \rightarrow \text{sentID});
239
                     if IMG_RAW then w_{\text{img}}(t) \leftarrow \text{mean}(\bar{\mathbf{a}}_t[I]);
240
                 end
241
                 /* --- Sentence aggregation ---
                                                                                                                                          */
242
                 foreach summary sentence g_i with token set T_i do
243
244
                      \mathcal{A}(j) \leftarrow \{i: \#\{t \in T_j: \hat{s}(t) = i\} \ge \lceil \tau |T_j| \rceil \};
245
                      if IMG_RAW then
246
                           compute W_{\text{img}}(j) = \frac{1}{|T_i|} \sum_{t \in T_i} w_{\text{img}}(t) for each g_j;
247
                           add IMG to sentence g_{i^*} with \max_i W_{img}(j)
249
                      if IMG_CAP then replace any i^* \in A(j) by IMG;
250
                 end
           end
251
```

Algorithm 1: Generation-time Source Attribution

3.3 Modes of Attribution

253 254

256257

258

259

260261

262

263

264

265

266267

268

269

While the three-stage pipeline defines a general recipe, the treatment of visual information requires distinct strategies. We therefore design two complementary modes that trade off direct fidelity to visual evidence against efficiency and text-only compatibility.

Text-only. The pipeline begins by splitting the source text into sentences and aligning tokens with their corresponding sentence IDs. During generation, each output token attends to the input sequence; we pool attentions and assign each token to its most attended source sentence. Sentence-level attribution is obtained by majority vote across tokens in the summary sentence. Details of ablation on different pipeline designs are discussed in Section 5.2.1.

Raw multimodal (IMG_RAW). For inputs containing both text and images, the source sequence includes a contiguous block of image tokens (one per merged patch). For each generated token, we sum its attention over all image tokens to obtain an image attribution score. At the sentence level,

we average these scores across all tokens in the sentence. The image is then attributed only to the summary sentence with the highest average image attention, in addition to any text spans.

Caption-as-image-span (IMG_CAP). As an alternative, we convert multimodal input to text-only by replacing each image placeholder with a one-sentence caption generated by the model. The caption span is treated as part of the source text during chunking. During inference, if a summary sentence is attributed to the caption span, we interpret this as an image citation. This mode removes the need for direct patch-level attention while preserving a textual trace to the visual evidence.

4 EXPERIMENTAL SETUP

4.1 Datasets

We evaluate on two representative clinical domains (Table 1): (i) CLICONSUMMATION (Tiwari et al., 2023), consisting of doctor–patient dialogues with both text-only and multimodal cases; and (ii) MIMIC-CXR (Johnson et al., 2019), where we use only the FINDINGS→IMPRESSION summarization task from textual reports after filtering. The final testbed is balanced across modalities, with 256 text-only and 263 multimodal examples, totaling 519.

Table 1: **Dataset statistics.** Breakdown of test sets used for evaluation. Examples and filtering criteria in Appendix B.

Dataset Domain		Selection	#Test Cases
CLICONSUMMATION MIMIC-CXR	Doctor–patient dialogues Radiology reports	100 text-only + 263 multimodal Findings \rightarrow Impression (filtered)	363 156
Total		256 text-only + 263 multimodal	519

4.2 BASELINES AND METRICS

All experiments are conducted with <code>Qwen2.5-VL-7B-Instruct</code> (Bai et al., 2025) and <code>LLaVA-Next</code> (Liu et al., 2024), two state-of-the-art open multimodal large language models. We enable attention outputs during generation in order to compute attribution without performing any additional training or fine-tuning.

We compare against two strong non-attention baselines:

Embedding similarity State-of-the-art sentence-BERT (Reimers & Gurevych, 2019) (all-MinilM-L6-v2) is used for text-text similarity and CLIP (Radford et al., 2021) (ViT-B-32) for text-image similarity. Each generated sentence is attributed to the most similar source sentences through thresholding, and to the image where similarity is maximal (see Appendix C for detailed implementation and hyperparameter tuning).

Model self-attribution. The same model that produces the summary is prompted to also generate citations, following the evaluation setup used for generating ground-truth labels.

We evaluate attribution quality along three dimensions: (i) **Text**: macro-averaged F1 and exact match of predicted vs. reference source sets; (ii) **Image**: accuracy of correctly citing the image; and (iii) **Joint**: exact match requiring both text and image elements to align.

4.3 IMPLEMENTATION DETAILS

Since gold-standard citations are unavailable, we construct a reference set using an LLM judge following Xie et al. (2024). For each generated sentence, the judge identifies the supporting source sentences (and image when present). This provides consistent supervision across systems while avoiding bias toward our own method. Prompt details are in Appendix E Hyperparameter choices for our attention-based pipeline (e.g., k for top-k pooling, sentence-level threshold τ , image scoring rules) are fixed across all experiments.

Table 2: **Attribution results.** Text-only results use majority voting with k=3, $\tau=0.16$ for Qwen2.5-VL-7B and k=5, $\tau=0.12$ for LLaVA-NeXT-7B; multimodal results are evaluated on 163 CLICONSUMMATION samples with the same hyperparameters.

	Text-only At		Attribution		Multimodal Attribution		
	Method	Macro-F1↑	Exact Match ↑	Text F1↑	Text EM ↑	Img Acc↑	Joint EM ↑
Qwen2.5-VL	Ours (Text)	76.33	58.70	-	-	_	_
	Ours (IMG_RAW)	_	_	65.52	30.75	75.47	26.46
	Ours (IMG_CAP)	_	_	58.37	38.52	77.85	34.87
	Sent-Embedding	72.14	41.72	53.21	10.86	76.53	8.48
	Self-Attribution	40.06	27.84	29.56	12.21	44.64	12.21
LLaVA-NeXT	Ours (Text)	62.28	23.33	-	-	_	_
	Ours (IMG_RAW)	_	_	49.37	13.32	81.49	18.12
	Ours (IMG_CAP)	_	_	56.31	28.02	65.13	21.39
	Sent-Embedding	63.85	13.52	57.11	25.40	73.77	17.65
	Self-Attribution	42.61	23.50	18.56	6.87	35.44	6.43

5 RESULTS AND ANALYSIS

We now turn to empirical evaluation of our attribution framework. Beyond simply reporting numbers, our goal is to analyze whether attention-based attribution can consistently outperform strong baselines across both text-only and multimodal summarization. We also ask whether different design choices such as how many tokens to aggregate or how to treat visual evidence, affect the stability and interpretability of the resulting citations.

5.1 MAIN RESULTS

5.1.1 Text-only Attribution

Table 2 reports results on the 256 text-only samples. Our attention-guided attribution substantially outperforms embedding- and generation-based baselines across both backbones.

For **Qwen2.5-VL-7B**, the best setting (majority voting, k=3, $\tau=0.16$) achieves **76.33** macro-F1 and **58.70** exact match, compared to 72.14 / 41.72 from Sentence-BERT and 40.06 / 27.84 from self-attribution. For **LLaVA-NeXT-7B**, our method still leads, attaining **62.28** macro-F1 and **23.33** exact match, versus 63.85 / 13.52 from Sentence-BERT. Although the margin is narrower for LLaVA-NeXT, our approach still provides stronger alignment and much higher exact match, highlighting that attention-guided attribution closes the gap between surface similarity and true grounding.

Notably, variants using "max" assignment collapse to below 13 F1 (see Table 4), underscoring that *majority voting over top-k attentions is crucial* for stable attributions.

5.1.2 MULTIMODAL ATTRIBUTION

Table 2 also summarizes results on the multimodal split. Both of our multimodal variants outperform all baselines across the two models.

For **Qwen2.5-VL-7B**, IMG_RAW achieves the strongest text grounding (65.52 F1) but weaker joint attribution, whereas IMG_CAP attains higher joint exact match (**34.87**) and image accuracy (**77.85**) while maintaining competitive text F1. For **LLaVA-NeXT-7B**, the pattern is consistent but less pronounced: IMG_CAP again yields stronger joint grounding (21.39 vs. 18.12), while IMG_RAW provides slightly higher standalone text F1 (49.37 vs. 56.31 for captions) and image accuracy (81.49).

This contrast highlights a practical trade-off:

- Raw patch-level attentions provide stronger standalone text grounding, but are more memoryintensive and less coherent across modalities.
- Caption-based attribution encourages more balanced evidence grounding across text and images, and is attractive for deployments where images cannot be stored or transmitted due to privacy concerns.

Baselines illustrate the limitations of alternatives. Sentence-BERT with CLIP embeddings achieves the highest image accuracy (80.53 for Qwen2.5-VL, 73.77 for LLaVA-NeXT) but fails at joint attribution (8.48 / 17.65). Self-attribution remains unreliable, performing poorly across all metrics.

Summary Across both backbones and input modalities, we observe three key findings: (1) majority voting is essential for converting noisy token-level attentions into stable sentence-level attributions; (2) attention-guided methods consistently outperform embedding and self-attribution baselines across both Qwen2.5-VL and LLaVA-NeXT; and (3) multimodal captioning provides a competitive alternative to raw-image attention, improving joint grounding while reducing complexity.

5.2 ABLATION STUDY

To ensure stability and to highlight the upper bound of our attribution framework, we perform the ablation studies on the stronger Qwen2.5-VL-7B backbone. As shown in Table 2, this model consistently outperforms LLaVA-NeXT-7B across both text-only and multimodal attribution, making it the most suitable candidate for analyzing the impact of hyperparameter choices in detail.

5.2.1 Hyperparameter Setting

We ablate three hyperparameters that govern attribution stability: (1) *Top-k tokens*: the number of most-attended source tokens considered per generated token; (2) *Attribution mode*: whether the token's source sentence is chosen by the single highest-attended token (max) or by majority voting over the top-k tokens (majority); (3) *Aggregation threshold* τ : the minimum proportion of tokens in a generated sentence that must support a source sentence for it to be retained as attribution. Low thresholds risk spurious matches, while high thresholds may discard true but sparse evidence.

All ablations are conducted on the text-only split to isolate hyperparameter effects from multimodal variability. Figure 2 visualizes the key findings (full numeric results are provided in Appendix D).

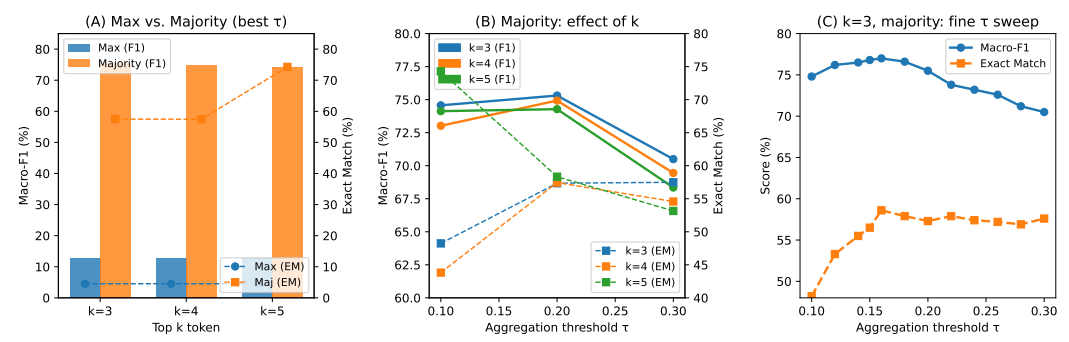


Figure 2: **Ablation on text-only attribution.** (A) Majority vs. Max (best τ per k): majority voting yields 60-point higher Macro-F1 and far stronger exact match than max, which collapses to near-random performance. (B) Effect of k under majority voting: attribution quality peaks around $\tau=0.2$, with k=3 providing the best balance between robustness and stability. (C) Fine-grained τ sweep for k=3, majority shows the optimal range lies between 0.15 and 0.18, supporting our choice of $\tau=0.16$ as the default setting. Full numeric results are provided in Appendix D.

Findings. Figure 2(A) contrasts max and majority modes. Across all values of k, max collapses to \sim 12 Macro-F1 and \sim 4.5 Exact Match, confirming that selecting the single strongest token is unstable and fails to capture distributed evidence. In contrast, majority consistently yields 60+point gains in F1, highlighting its robustness.

Figure 2(B) explores the effect of τ under majority voting. For $k \in \{3,4,5\}$, performance peaks around $\tau = 0.2$: lower thresholds admit spurious matches, while higher thresholds prune true but sparse support. Although larger k sometimes improves exact match (e.g., k = 5), it dilutes F1 and leads to less stable attribution, whereas k = 3 balances robustness and efficiency.

Finally, Figure 2(C) zooms in on a fine-grained sweep for k=3, majority. Here, Macro-F1 reaches its maximum at $\tau=0.15$ –0.16 (76.4 F1), while Exact Match peaks at $\tau=0.16$ (58.70). This validates $\tau\approx0.18$ as a robust default.

Choice of final hyperparameters. Based on these results, we adopt k=3, majority, $\tau=0.16$ as our default configuration. This setting achieves the best trade-off (76.33 Macro-F1 / 58.70 Exact Match) and consistently outperforms both embedding-based and self-attribution baselines.

Implications. These results show that attribution stability depends not only on raw attention scores but also on how they are aggregated. Majority-based aggregation with a small top-k acts as a denoising mechanism, turning noisy token-level distributions into reliable sentence-level citations. Beyond our datasets, this suggests a general recipe for applying attention-based attribution: restrict to a focused set of tokens, use majority voting to stabilize decisions, and adopt moderate thresholds to balance recall and precision. Together, these design choices transform raw attentions—often dismissed as uninterpretable—into a practical tool for generating faithful, human-auditable citations.

5.2.2 Does Better Attribution Lead to Better Summaries?

Table 3: Summary quality evaluation with Qwen-7B under different multimodal settings.

Mode	ROUGE-1	ROUGE-L	BERTScore-F1
IMG_RAW	0.537	0.400	0.913
IMG_CAP	0.496	0.374	0.902

We further examine whether attribution quality correlates with summary quality. Table 3 reports the summary evaluation results of <code>Qwen-2.5-7B</code> under different multimodal settings, comparing raw image input against caption input.

Analysis. From Table 3, using raw images yields better summary quality than captioning (+4.1 ROUGE-1, +2.6 ROUGE-L, +1.1 BERTScore-F1). This trend aligns with the multimodal attribution results in Table 2, where raw-image attribution achieved stronger text F1 compared to caption-based attribution. Although caption-based attribution produced higher text EM and joint EM, raw images consistently provide higher overall summary fidelity.

These findings highlight a trade-off: **Raw images** enable stronger alignment with the reference text and better overall summary metrics, at the cost of slightly lower robustness in exact span matches. **Caption input** may guide models toward more precise sentence-level matches (higher EM in Table 2), but at the expense of degraded semantic fidelity in summaries.

Overall, attribution quality does exhibit correlation with summary quality: better multimodal attribution (raw images) coincides with improved semantic summary metrics, suggesting that robust attribution mechanisms enhance the informativeness and grounding of generated summaries.

6 Discussion & Insights

Our study yields several practical takeaways. First, in clinical summarization tasks, caption-based attribution emerges as a lightweight yet effective alternative to raw image attention. This is particularly useful in scenarios where images cannot be shared or processed directly, but textual surrogates are feasible. Second, generating source citations alongside summaries improves trustworthiness: clinicians can see not only what the model outputs, but also where each statement comes from. This aligns with broader goals of transparency and safety in clinical AI. At the same time, our approach highlights opportunities for reproducibility and deployment. Because it is training-free and model-agnostic, the method can be readily plugged into existing pipelines for auditing and validation.

Limitations remain. Attributions rely on alignment between attention weights and true evidence, and our evaluation is restricted to two datasets. Future work will extend to larger clinical corpora, explore domain-tuned models, and investigate real-world deployment in clinical workflows.

ETHICS STATEMENT

This work focuses on attribution and grounding for multimodal clinical summarization. We emphasize that our experiments are conducted on publicly available benchmark datasets (e.g., MIMIC-CXR and CliConSummation) that have undergone de-identification and institutional review, ensuring no personally identifiable patient data is used. All methods are designed for research purposes only and are not intended for direct clinical deployment without additional validation and regulatory approval. We acknowledge that automatic summarization and attribution in healthcare carries potential risks, including the possibility of generating misleading or incomplete explanations. To mitigate these risks, we stress that outputs should be interpreted as research findings rather than medical advice. We do not foresee conflicts of interest or sponsorship concerns in this work.

REPRODUCIBILITY STATEMENT

We have taken multiple steps to ensure the reproducibility of our results. All hyperparameter choices and evaluation protocols are documented in the main text (e.g. Section 5.2.1) and the Appendix (e.g. Appendix D, E). We provide complete descriptions of dataset construction and preprocessing in Appendix B. To facilitate replication, our attribution code and evaluation scripts will be made available in the supplementary materials during the review process. Further, ablation studies (Appendix D) provide insight into the sensitivity of our method to hyperparameters, and additional results across two backbones (Qwen2.5-VL and LLaVA-NeXT) demonstrate robustness. Together, these resources support faithful reproduction and extension of our findings.

REFERENCES

- Chirag Agarwal, Alon Johnson, Sara Hooker, Osbert Bastani, Been Kim, John Langford, Eric Wallace, and Osbert Bastani. Openxai: Towards a transparent evaluation of model explanations. In *Advances in Neural Information Processing Systems*, 2022. URL https://arxiv.org/abs/2206.11104.
- Shuai Bai, Keqin Chen, Xuejing Liu, Jialin Wang, Wenbin Ge, Sibo Song, Kai Dang, Peng Wang, Shijie Wang, Jun Tang, et al. Qwen2. 5-vl technical report. *arXiv preprint arXiv:2502.13923*, 2025.
- Saahil Jain, Ashwin Agrawal, Adriel Saporta, Steven QH Truong, Du Nguyen Duong, Tan Bui, Pierre Chambon, Yuhao Zhang, Matthew P Lungren, Andrew Y Ng, et al. Radgraph: Extracting clinical entities and relations from radiology reports. *arXiv* preprint arXiv:2106.14463, 2021.
- Alistair EW Johnson, Thomas J Pollard, Seth J Berkowitz, Nathaniel R Greenbaum, Matthew P Lungren, Charles Y Deng, Roger G Mark, Steven Horng, and Leo Anthony Celi. Mimic-cxr, a de-identified publicly available database of chest radiographs with free-text reports. *Scientific data*, 6(1):317, 2019.
- Hita Kambhamettu, Jamie Flores, and Andrew Head. Traceable text: Deepening reading of aigenerated summaries with phrase-level provenance links. *arXiv preprint arXiv:2409.13099*, 2024.
- Vladimir Karpukhin, Barlas Oguz, Sewon Min, Patrick Lewis, Ledell Wu, Sergey Edunov, Danqi Chen, and Wen-tau Yih. Dense passage retrieval for open-domain question answering. In *Proceedings of the 2020 Conference on Empirical Methods in Natural Language Processing (EMNLP)*, pp. 6769–6781, 2020. URL https://aclanthology.org/2020.emnlp-main.550.
- Omar Khattab and Matei Zaharia. Colbert: Efficient and effective passage search via contextualized late interaction over bert. *Proceedings of the 43rd International ACM SIGIR Conference on Research and Development in Information Retrieval*, pp. 39–48, 2020. doi: 10.1145/3397271. 3401075.
- Philippe Laban, Tobias Schnabel, Paul N. Bennett, and Marti A. Hearst. SummaC: Re-visiting NLI-based models for inconsistency detection in summarization. *Transactions of the Association for Computational Linguistics*, 10:163–177, 2022. doi: 10.1162/tacl_a_00453. URL https://aclanthology.org/2022.tacl-1.10/.

- Mingzhe Li, Xiuying Chen, Shen Gao, Zhangming Chan, Dongyan Zhao, and Rui Yan. VMSMO: Learning to generate multimodal summary for video-based news articles. In Bonnie Webber, Trevor Cohn, Yulan He, and Yang Liu (eds.), *Proceedings of the 2020 Conference on Empirical Methods in Natural Language Processing (EMNLP)*, pp. 9360–9369, Online, November 2020. Association for Computational Linguistics. doi: 10.18653/v1/2020.emnlp-main.752. URL https://aclanthology.org/2020.emnlp-main.752/.
- Haotian Liu, Chunyuan Li, Yuheng Li, Bo Li, Yuanhan Zhang, Sheng Shen, and Yong Jae Lee. Llava-next: Improved reasoning, ocr, and world knowledge, January 2024. URL https://llava-vl.github.io/blog/2024-01-30-llava-next/.
- Potsawee Manakul, Adian Liusie, and Mark Gales. SelfCheckGPT: Zero-resource black-box hallucination detection for generative large language models. In Houda Bouamor, Juan Pino, and Kalika Bali (eds.), *Proceedings of the 2023 Conference on Empirical Methods in Natural Language Processing*, pp. 9004–9017, Singapore, December 2023. Association for Computational Linguistics. doi: 10.18653/v1/2023.emnlp-main.557. URL https://aclanthology.org/2023.emnlp-main.557/.
- Kevin Meng, David Bau, Alex Andonian, and Yonatan Belinkov. Locating and editing factual associations in gpt. *Advances in neural information processing systems*, 35:17359–17372, 2022.
- Sourajit Mukherjee, Anubhav Jangra, Sriparna Saha, and Adam Jatowt. Topic-aware multimodal summarization. In Yulan He, Heng Ji, Sujian Li, Yang Liu, and Chua-Hui Chang (eds.), *Findings of the Association for Computational Linguistics: AACL-IJCNLP 2022*, pp. 387–398, Online only, November 2022. Association for Computational Linguistics. doi: 10.18653/v1/2022.findings-aacl. 36. URL https://aclanthology.org/2022.findings-aacl.36/.
- Dang Nguyen, Chacha Chen, He He, and Chenhao Tan. Pragmatic radiology report generation. In *Machine Learning for Health (ML4H)*, pp. 385–402. PMLR, 2023.
- Alec Radford, Jong Wook Kim, Chris Hallacy, Aditya Ramesh, Gabriel Goh, Sandhini Agarwal, Girish Sastry, Amanda Askell, Pamela Mishkin, Jack Clark, Gretchen Krueger, and Ilya Sutskever. Learning transferable visual models from natural language supervision. In *International Conference on Machine Learning*, 2021. URL https://api.semanticscholar.org/CorpusID: 231591445.
- Nils Reimers and Iryna Gurevych. Sentence-bert: Sentence embeddings using siamese bert-networks. In *Conference on Empirical Methods in Natural Language Processing*, 2019. URL https://api.semanticscholar.org/CorpusID:201646309.
- Phillip Sloan, Phillip Clatworthy, Edwin Simpson, and Majid Mirmehdi. Automated radiology report generation: A review of recent advances. *IEEE Reviews in Biomedical Engineering*, 18:368–387, 2024.
- Yoshi Suhara and Dimitris Alikaniotis. Source identification in abstractive summarization. In Yvette Graham and Matthew Purver (eds.), *Proceedings of the 18th Conference of the European Chapter of the Association for Computational Linguistics (Volume 2: Short Papers)*, pp. 212–224, St. Julian's, Malta, March 2024. Association for Computational Linguistics. doi: 10.18653/v1/2024. eacl-short.20. URL https://aclanthology.org/2024.eacl-short.20/.
- Abhisek Tiwari, Anisha Saha, Sriparna Saha, Pushpak Bhattacharyya, and Minakshi Dhar. Experience and evidence are the eyes of an excellent summarizer! towards knowledge infused multi-modal clinical conversation summarization. In *Proceedings of the 32nd ACM International Conference on Information and Knowledge Management*, pp. 2452–2461, 2023.
- Min Xiao, Junnan Zhu, Feifei Zhai, Chengqing Zong, and Yu Zhou. Pay more attention to images: Numerous images-oriented multimodal summarization. In Luis Chiruzzo, Alan Ritter, and Lu Wang (eds.), *Proceedings of the 2025 Conference of the Nations of the Americas Chapter of the Association for Computational Linguistics: Human Language Technologies (Volume 1: Long Papers)*, pp. 9379–9392, Albuquerque, New Mexico, April 2025. Association for Computational Linguistics. ISBN 979-8-89176-189-6. doi: 10.18653/v1/2025.naacl-long.474. URL https://aclanthology.org/2025.naacl-long.474/.

Yiqing Xie, Sheng Zhang, Hao Cheng, Pengfei Liu, Zelalem Gero, Cliff Wong, Tristan Naumann, Hoifung Poon, and Carolyn Rose. DocLens: Multi-aspect fine-grained evaluation for medical text generation. In Lun-Wei Ku, Andre Martins, and Vivek Srikumar (eds.), *Proceedings of the 62nd Annual Meeting of the Association for Computational Linguistics (Volume 1: Long Papers)*, pp. 649–679, Bangkok, Thailand, August 2024. Association for Computational Linguistics. doi: 10. 18653/v1/2024.acl-long.39. URL https://aclanthology.org/2024.acl-long.39/.

Jin Xu, Xiaoqian Luo, and Buzhou Tang. Interpretability of clinical decision support systems: a survey. *Journal of Healthcare Informatics Research*, 2023. doi: 10.1007/s41666-023-00154-0.

Junnan Zhu, Haoran Li, Tianshang Liu, Yu Zhou, Jiajun Zhang, and Chengqing Zong. MSMO: Multimodal summarization with multimodal output. In Ellen Riloff, David Chiang, Julia Hockenmaier, and Jun'ichi Tsujii (eds.), *Proceedings of the 2018 Conference on Empirical Methods in Natural Language Processing*, pp. 4154–4164, Brussels, Belgium, October-November 2018. Association for Computational Linguistics. doi: 10.18653/v1/D18-1448. URL https://aclanthology.org/D18-1448/.

A APPENDIX

B DATA PREPROCESSING AND FILTERING FOR MIMIC-CXR

To construct a reliable text-only test set from MIMIC-CXR, we applied several filtering steps to the raw reports:

Step 1: Identify single-report patients. We first traversed the report directory and grouped all reports by patient ID. Only patients with a single report were retained to avoid complications where impressions referenced prior studies.

```
for patient_id in all_patients:
    if len(reports[patient_id]) == 1:
        keep patient id
```

Step 2: Extract FINDINGS and IMPRESSION sections. From each retained report, we extracted the FINDINGS and IMPRESSION sections using regex patterns. Reports missing either section were discarded.

Step 3: Sentence-length filtering. We segmented both sections into sentences and required a minimum of ≥ 9 sentences in FINDINGS and ≥ 5 sentences in IMPRESSION. This ensured enough content for meaningful summarization.

```
if len(sent(FINDINGS)) >= 9
and len(sent(IMPRESSION)) >= 5:
    keep report
```

Outcome. This pipeline produced **156** text-only test cases. Together with CLICONSUMMATION, our combined evaluation set is modality-balanced (256 text-only, 263 multimodal, total 519 examples).

C BASELINE IMPLEMENTATION DETAILS

For comparison, we implemented a simple *embedding-based attribution baseline* that relies on pretrained encoders. The method operates in two stages:

• **Text-text similarity.** Both source sentences and generated summary sentences are encoded in a text embedding space (we used a Sentence-BERT variant). Cosine similarity is computed to rank candidate source sentences for each generated sentence.

649

650

651 652

653

654

655

656 657 • **Text-image similarity.** When an image is present, generated sentences are additionally embedded in the CLIP text space, and compared against the CLIP embedding of the image. The image is assigned to the generated sentence with the highest text-image similarity.

Each generated sentence is then attributed to the subset of source sentences exceeding a cosine similarity threshold, together with the image if applicable. If the image is selected, it is always enforced to appear at most once per summary, assigned to the most relevant generated sentence. We experimented with different similarity thresholds and report in the main paper only the *best-performing configuration*.

Below we include the implementation used for this baseline.

```
658
      from sentence_transformers import SentenceTransformer
659
      import torch, torch.nn.functional as F
660
      from PIL import Image
      from typing import List, Union
662
      class MultimodalAttributionModel:
663
         def __init__(self,
664
             text_model_name: str = "TEXT_ENCODER", # text2text encoder
665
            clip_model_name: str = "CLIP_ENCODER", # text2image shared encoder
666
            threshold_text: float = 0.5,
            max\_sources: int = 10,
667
            img_counts_towards_k: bool = True):
668
            self.text_model = SentenceTransformer(text_model_name)
669
            self.clip_model = SentenceTransformer(clip_model_name)
670
            self.threshold text = threshold text
671
             self.max_sources = max_sources
             self.img_counts_towards_k = img_counts_towards_k
672
673
          @torch.no grad()
674
          def _embed_text_textspace(self, sentences):
675
             return self.text_model.encode(
676
                sentences, convert_to_tensor=True, normalize_embeddings=True)
677
          @torch.no_grad()
678
         def _embed_text_clipspace(self, sentences):
679
             return self.clip_model.encode(
680
                sentences, convert_to_tensor=True, normalize_embeddings=True)
681
          @torch.no_grad()
682
          def _embed_image_clipspace(self, image_path: str):
683
            img = Image.open(image_path).convert("RGB")
684
            emb = self.clip_model.encode([img],
685
                 convert_to_tensor=True, normalize_embeddings=True)
686
             return emb[0] # [d]
687
          def attribute(self, source_sentences: List[str],
688
                    generated_sentences: List[str],
689
                     image_path: Union[str, None] = None):
690
             # (1) text2text similarities
             src_emb = self._embed_text_textspace(source_sentences)
691
            gen_emb = self._embed_text_textspace(generated_sentences)
692
            sim_text = F.cosine_similarity(
693
                gen_emb.unsqueeze(1), src_emb.unsqueeze(0), dim=-1)
694
695
             # (2) text2image similarity (CLIP), if image present
696
            have_img = image_path is not None
            if have imq:
697
                img_emb = self._embed_image_clipspace(image_path)
698
                gen_emb_clip = self._embed_text_clipspace(generated_sentences)
699
                sim_img = F.cosine_similarity(gen_emb_clip,
700
                        img_emb.unsqueeze(0), dim=-1)
                img_best_idx = int(torch.argmax(sim_img).item())
             else:
```

```
702
                img\_best\_idx = -1
703
             # (3) attribution assignment
             attributions = []
705
             for i in range(len(generated_sentences)):
706
                sim_row = sim_text[i]
707
                sorted_sims, sorted_idxs = torch.sort(sim_row, descending=True)
708
709
                chosen = []
710
                for sim, idx in zip(sorted_sims, sorted_idxs):
                   if sim.item() >= self.threshold_text:
711
                      chosen.append(int(idx.item()))
712
                   if len(chosen) >= self.max_sources:
713
                      break
714
                # enforce IMG to appear once
715
                if have_img and i == img_best_idx:
716
                   if len(chosen) >= self.max_sources:
717
                       chosen = chosen[: self.max_sources - 1]
718
                   chosen.append("IMG")
719
720
                attributions.append(chosen)
721
             return attributions
722
723
```

D ABLATION RESULTS

Here we provide the numerical results of our ablation study in Table 4.

E PROMPT DETAILS FOR THE GPT ANNOTATOR

We employed GPT-based annotation to construct silver reference attributions. The same prompts were also used when implementing the *self-attribution* baseline, where the model that generated the summaries was asked to directly output source citations.

763 764 765 766 Table 4: Ablation on text-only attribution. Bold highlights best values. 767 Top-k Attr mode Agg. τ Macro-F1 **Exact Match** 768 769 3 0.1 12.58 4.54 max 770 3 12.58 4.54 max 0.2 771 3 0.3 12.58 4.54 max 772 3 0.10 74.57 48.24 majority 773 3 75.81 53.27 majority 0.12 774 3 55.31 0.1476.18 majority 775 3 majority 0.15 76.43 56.51 776 3 58.70 majority 0.16 76.33 777 3 0.18 75.77 57.77 majority 778 3 0.20 75.31 57.35 majority 779 3 0.22 73.56 57.93 majority 780 3 majority 0.24 72.97 57.35 781 3 majority 0.25 72.81 57.35 782 3 72.34 57.18 0.26 majority 783 3 0.28 71.04 56.93 majority 784 3 0.30 70.50 57.49 majority 785 4 max 0.1 12.78 4.54 786 4 max 0.2 12.78 4.54 787 4 0.3 12.78 4.54 max 788 4 0.1 73.02 43.82 majority 789 4 0.2 74.93 57.45 majority 790 4 69.45 54.58 majority 0.3 791 5 0.1 12.78 4.54 max 792 5 0.2 12.78 4.54 max 793 5 0.3 12.78 4.54 max 794 5 0.1 74.13 74.28 majority 795 5 0.2 74.28 58.34 majority 796 5 0.3 68.35 53.15 majority 797 798 Ours (best) Top-k=3, Majority, $\tau=0.16$ 76.33 58.70 799 Baseline: Sent_emb 72.14 41.72 800 Baseline: Self_attr 40.06 27.84

```
810
811
812
           You are given a list of source sentences and a list of generated sentences from the summary. For each
813
           generated sentence, identify one or more source sentences it can be attributed to based on semantic
814
           similarity and information content.
           Input Format:
815
816
           Source Sentences:
           [0] sentence 1
817
           [1] sentence 2
818
819
820
           Generated Sentences:
           [0] generated sentence 1
821
           [1] generated sentence 2
822
           . . .
823
           Output Format:
824
           [0] [source sentence ids]
825
           [1] [source sentence ids]
826
827
           Example:
828
           Source Sentences:
829
           [0] The patient has a fever.
830
           [1] The patient complains of headache.
831
832
           Generated Sentences:
833
           [0] The patient is experiencing fever
           and headache.
834
835
           Output:
836
           [0] [0, 1]
837
           Now attribute the following:
838
           Source Sentences:
839
           {source}
840
841
           Generated Sentences:
842
           {summary}
843
           Output:
844
845
```

```
864
865
866
           You are given a list of source sentences (the text contains an "¡image¿" placeholder) and one associated
867
           image. For each generated summary sentence, identify the source elements (sentences and/or image) it
           can be attributed to.
868
           Input Format:
869
           Source Sentences:
870
           [0] source sentence 1
871
           [1] source sentence 2
872
873
874
           Generated Sentences:
           [0] generated sentence 1
875
           [1] generated sentence 2
876
           . . .
877
           Output Format:
878
           [0] [source ids and/or IMG]
879
           [1] [source ids and/or IMG]
880
881
           Example:
882
           Image shows a red eye.
883
           Source Sentences:
884
           [0] Doctor: Do you have eye pain?
885
           [1] Patient: Yes, my right eye is very red.
886
           <image>
887
           Generated Sentences:
888
           [0] The patient has eye redness.
889
890
           Output:
891
           [0] [1, IMG]
892
           Now attribute the following:
893
           Source Sentences:
894
           {source}
895
896
           Generated Sentences:
897
           {summary}
898
           Output:
899
900
```